THYROID
Volume 24, Number 11, 2014

DOI: 10.1089/thy.2014.0169

A Thyroid Hormone Challenge in Hypothyroid Rats Identifies T3 Regulated Genes in the Hypothalamus and in Models with Altered Energy Balance and Glucose Homeostasis

Annika Herwig,[1,2] Gill Campbell,[1] Claus-Dieter Mayer,[3] Anita Boelen,[4] Richard A. Anderson,[1] Alexander W. Ross,[1] Julian G. Mercer,[1] and Perry Barrett[1]

Background: The thyroid hormone triiodothyronine (T3) is known to affect energy balance. Recent evidence points to an action of T3 in the hypothalamus, a key area of the brain involved in energy homeostasis, but the components and mechanisms are far from understood. The aim of this study was to identify components in the hypothalamus that may be involved in the action of T3 on energy balance regulatory mechanisms.
Methods: Sprague Dawley rats were made hypothyroid by giving 0.025% methimazole (MMI) in their drinking water for 22 days. On day 21, half the MMI-treated rats received a saline injection, whereas the others were injected with T3. Food intake and body weight measurements were taken daily. Body composition was determined by magnetic resonance imaging, gene expression was analyzed by *in situ* hybridization, and T3-induced gene expression was determined by microarray analysis of MMI-treated compared to MMI-T3-injected hypothalamic RNA.
Results: *Post mortem* serum thyroid hormone levels showed that MMI treatment decreased circulating thyroid hormones and increased thyrotropin (TSH). MMI treatment decreased food intake and body weight. Body composition analysis revealed reduced lean and fat mass in thyroidectomized rats from day 14 of the experiment. MMI treatment caused a decrease in circulating triglyceride concentrations, an increase in nonesterified fatty acids, and decreased insulin levels. A glucose tolerance test showed impaired glucose clearance in the thyroidectomized animals. In the brain, *in situ* hybridization revealed marked changes in gene expression, including genes such as *Mct8*, a thyroid hormone transporter, and *Agrp*, a key component in energy balance regulation. Microarray analysis revealed 110 genes to be up- or downregulated with T3 treatment (± 1.3-fold change, $p < 0.05$). Three genes chosen from the differentially expressed genes were verified by *in situ* hybridization to be activated by T3 in cells located at or close to the hypothalamic ventricular ependymal layer and differentially expressed in animal models of long- and short-term body weight regulation.
Conclusion: This study identified genes regulated by T3 in the hypothalamus, a key area of the brain involved in homeostasis and neuroendocrine functions. These include genes hitherto not known to be regulated by thyroid status.

Introduction

The hypothalamus is an important region of the central nervous system for the control of energy balance, integrating both peripheral and central signals before gating an appropriate response via neuroendocrine or sympathetic outputs to achieve physiological homeostasis. A component of the energy balance system is the thyroid hormone triiodothyronine (T3), whose level in the circulation is monitored by the hypothalamus (1). T3 has long been known to affect metabolism and body weight in mammals profoundly, including humans (2–4). Patients suffering from thyroid dysfunctions often struggle to maintain a stable energy balance. Hypothyroidism has been linked to obesity and the metabolic

[1]Ingestive Behaviour Group; [3]Biomathematics and Statistics Scotland; Rowett Institute for Nutrition and Health, University of Aberdeen, Aberdeen, United Kingdom.
[2]Zoological Institute, University of Hamburg, Hamburg, Germany.
[4]Department of Endocrinology, Metabolism, Academic Medical Center, University of Amsterdam, Amsterdam, The Netherlands.

syndrome, while, at the other extreme, hyperthyroidism can lead to weight loss, insulin resistance, and glucose intolerance as a result of thyrotoxicosis (4–7). Until recently, the effects of T3 on energy balance were thought to be mainly mediated by the hormone's action directly in peripheral tissues. In brown adipose tissue and skeletal muscle, T3 regulates the activity of uncoupling proteins and thereby triggers thermogenesis, an important factor in energy expenditure (8,9). However, besides controlling metabolism in peripheral tissues, increasing evidence exists for T3 action directly within the brain to regulate central pathways of appetite and metabolism (10–13).

Thyroid hormones are produced in the thyroid gland and are released into the circulation from where they are shuttled to the brain via at least two identified highly specific transporters: the organic anion transporting polypeptide 1c1 (OATP1C1) and the monocarboxylate transporter 8 (MCT8) (14–16). Thyroxine (T4), the precursor of T3, is released by the thyroid gland and is under the tight control of an autoregulatory feedback system involving the paraventricular nucleus of the hypothalamus and the pituitary (17). T3 is predominantly derived from T4 by the action of type II deiodinase (DIO2) and type I deiodinase (DIO1) in any given target tissue.

Three deiodinase enzymes have been identified. However, only two of them are present in the brain where they locally regulate T3 levels: DIO2 activates T4 to T3 by outer ring deiodination, whereas type III deiodinase (DIO3) catalyzes inner ring deiodination of T4 or T3 to the inactive forms of reverse T3 (rT3) or 3,3′-diidothyronine (T2) respectively. Hence, whereas DIO2 increases T3 availability, DIO3 is the enzyme involved in limiting or reducing T3 availability and action (18,19). Within the hypothalamus—the brain area involved in the homeostatic control of energy balance—both deiodinase enzymes are highly expressed in ependymal/tanycyte cells lining the third ventricle (20,21).

In ventricular ependymal/tanycyte cells, deiodinase expression and activity is strongly altered in response to short-term energetic challenges such as fasting or critical illness, but also when long-term shifts in energy balance occur, as in seasonal mammals (20–26). Importantly, the local changes in thyroid hormone metabolism in ventricular ependymal cells appear to be partially independent of the hypothalamus-pituitary-thyroid (HPT) axis and thyroid hormone status in the periphery (27,28). It is assumed that once locally activated by DIO2 in tanycytes—specialized glial cells of the ependymal layer—T3 can directly act on neuronal pathways within the hypothalamus and thereby centrally influence food intake and energy expenditure (11–13,22).

Consistent with the functional evidence for T3 involvement in the central regulation of energy balance, knockout mice with defective thyroid hormone receptors show impaired metabolism, body weight, glucose, and lipid handling (29), while several studies using either *in situ* hybridization or immunocytochemistry have demonstrated an appropriate distribution of thyroid hormone receptor isoforms in energy balance–related nuclei in the hypothalamus of several species, including humans (20,30,31).

Taken together, the available evidence supports thyroid hormone action in the hypothalamus acting on mechanisms that affect energy balance in mammals. However, we know comparatively little about the molecular mechanisms and pathways that are regulated by thyroid hormone in the brain to regulate homeostatic mechanisms.

In this study, we screened for mechanisms of T3 action on appetite and energy balance regulatory mechanisms in the hypothalamus by comparing hypothalamic gene expression by microarray analysis between chemically induced hypothyroid Sprague Dawley rats with and without T3 administration. We then applied the information derived from the microarray studies to the analysis of gene expression in two models of altered short-term or long-term energy balance: the fasted and re-fed rat, and the Siberian hamster under long day and short day photoperiod.

Material and Methods

All research using animals was licensed under the Animals Act of 1986 (Scientific Procedures) and received ethical approval from the Rowett Research Institute ethical review committee.

Male Sprague Dawley rats were purchased from Charles River UK at the age of six weeks. Rats were kept in a 12h:12h light dark cycle at 21 ± 2°C and acclimatized for one week. A standard pelleted diet and water were available *ad libitum*.

Chemically induced hypothyroidism

Throughout the study, food intake and body weight were monitored daily, and body composition was assessed on all animals at days 0, 7, 14, and 21 using a nuclear magnetic resonance scanner (EchoMRI, Houston, TX). From day 1 of the experiment, two cohorts of rats were made hypothyroid by supplementing their drinking water with 0.025% of the thyroperoxidase inhibitor methimazole (MMI) and 3% saccharin for 22 days ($n = 48$). Water containing MMI and saccharin was freshly prepared and changed every second day. To achieve minimum possible circulating thyroid hormone levels, iopanoic acid (IOP; 100 mg/kg) was injected at days 1, 7, 14, and 21 to inhibit deiodinase activity. On day 21 of the experiment, half the hypothyroid rats received a 25 μg/100 g intraperitoneal (i.p.) T3 injection (group MMI-T3, $n = 24$), whereas the other half were injected with saline (group MMI-sal, $n = 24$).

A third group of rats without MMI treatment received a saline injection on day 21 and served as a naïve control group (control, $n = 20$). Twenty-four hours after T3 or saline injection (day 22), animals were anaesthetized using isoflurane inhalation and then decapitated. Trunk blood was collected for serum preparation, and the brains were removed and frozen on dry ice. Serum and brains were stored at -70°C until required.

A second identical experiment investigated glucose tolerance in the chemically induced hypothyroid animals. A glucose tolerance test was performed in control animals ($n = 6$) and MMI-treated animals ($n = 12$) on day 20 of the experiment. Glucose at 1 g/kg body weight was injected i.p., and blood samples were taken from the tail vein at 0, 7, 15, 30, 90, and 120 min after injection. Serum was stored at -70°C until further analysis.

Serum analysis

Serum levels of T3, T4, and thyrotropin (TSH) were determined by in-house radioimmunoassays (32,33). Glucose,

NEFAs, and triglycerides were assayed using the Konelab 30 clinical chemistry analyzer, and serum insulin concentrations using a rat insulin enzyme-linked immunosorbent assay (ELISA; Mercodia, Uppsala, Sweden).

Microarray analysis

Hypothalamic blocks spanning the ARC (Bregma −2.12 mm to −4.52 mm) were cut from frozen brains, and total RNA was extracted from individual blocks by homogenization in Trizol. RNA was treated with DNase to eliminate any contaminating DNA and purified using Qiagen RNAeasy spin columns. RNA integrity was assessed using the Agilent Bioanalyzer Lab-On-a-Chip analysis system (Agilent Technologies, Santa Clara, CA). RNA was amplified in two steps to cRNA, incorporating Cy-3 and Cy-5 dyes, and was purified with RNeasy mini spin columns. Labeled RNA from individual hypothalamic blocks was applied in MMI-T3 ($n=4$) versus MMI-sal ($n=4$) pairs to Agilent rat whole genome microarrays. Gene expression microarrays (4x44K) were manufactured and supplied by Agilent Technologies, and contained 60-mer probes with approximately 30,000 Entrez Gene RNAs represented. Labeled cRNA was hybridized to each array rotating at 65°C for 17 h. After washing, the arrays were scanned using a SureScan High Resolution Scanner (Agilent Technologies).

The statistical programming language R (v3.0.2) was used to analyze the raw expression data. Gene expression values were analyzed on log2 scale, and Loess normalization was conducted to remove an overall intensity depending dye effect using the Bioconductor library limma (v3.18.9). Values of spots that were represented by identical oligos were averaged across duplicates. The limma package was also used to detect the most significant gene expression changes using a linear model with the factors dye (Cy3, Cy5) and treatment (saline, T3). The *p*-values for the treatment effect were adjusted for multiple testing by using the Benjamini–Hochberg method, and probes with an adjusted *p*-value below 0.25 were deemed significant (corresponding to a false discovery rate of 25%). In order not to overlook biologically relevant large but not quite so statistically significant changes, probes that displayed a change of twofold or more in either direction and had a *p*-value of <0.01 were also added this list. Log2 ratios of treatment effects were back transformed to obtain fold changes. The data discussed in this publication have been deposited in NCBI's Gene Expression Omnibus (34) and are accessible through GEO Series accession number GSE55803 (www.ncbi.nlm.nih.gov/geo/query/acc.cgi?acc=GSE55803).

Fasted and re-fed rats

To investigate expression changes of candidate genes in additional animal models of energy balance, two further experiments were carried out. First, a rat model of short-term energy deficit (fasting) with subsequent re-feeding was studied. Male Sprague Dawley rats were purchased from Charles River UK at the age of eight weeks. They were kept in a 12h:12h light dark cycle at 21 ± 2°C and acclimatized for one week. A standard pelleted diet and water were available *ad libitum*. One group ($n=8$ per group) of rats was then fasted for 48 h. A second group was fasted for 48 h and then re-fed for 24 h, and a third group was fed *ad libitum* throughout as control. Animals were killed at ZT3 (3 h after lights on). Their brains were dissected, frozen on dry ice, and maintained at −70°C until further use.

Long day and short day acclimatized Siberian hamsters

Siberian hamsters were drawn from a colony at the Rowett Institute for Nutrition and Health, University of Aberdeen, bred and raised under long day (LD; 16:8 h light:dark) conditions. At the age of three months, hamsters were either exposed to LD ($n=6$) or short day (SD; 8:16 h light:dark, $n=7$) conditions. Animals were housed individually, food (standard pellet diet) and water were available *ad libitum* throughout the entire experiment, and ambient temperature was maintained at 22°C. Body weight was monitored weekly. After 14 weeks, hamsters were killed at ZT3 by cervical dislocation. Brains were dissected, frozen on dry ice, and stored at −70°C until required.

Cloning of riboprobes and in situ *hybridization*

Messenger RNA levels and distribution of selected genes regulated by T3 were analyzed in coronal hypothalamic sections by *in situ* hybridization. Twenty micron–thick sections of the hypothalamus were cut and mounted onto poly-L-lysine coated slides. Every tenth section was mounted onto a slide to generate 10 slide sets (two slides per rat) with representative sections spanning the hypothalamic region containing the arcuate nucleus (Bregma −1.72 mm to −4.08 mm) or the paraventricular nucleus (Bregma −0.24 mm to −1.78 mm, Paxinos and Watson, The rat brain). Riboprobes were generated from cloned polymerase chain reaction (PCR)-generated fragments for *Dio2*, *Dio3*, *Mct8*, *Trh*, *Npy*, *Pomc*, *Agrp*, as previously described (25, 26, 35–37). Probes for *Hairless, Sned1*, and *Plunc* were cloned using rat hypothalamic cDNA with the following primers: for *Hairless*, primers were based on Genbank sequence (NM_024364), forward primer 5′-CAC TGG GCT CCG GGC ACT CAA G-3′ (bases 1667–1688), reverse primer 5′-TGC CTG GGC TGT CCT CTG TCA T-3′ (bases 2223–2202); *Sned1* primers based on Genbank sequence (AF439716), forward primer 5′-AGC CTG CGC ACC TCT ACA TCA TCA-3′ (bases 2214–2233); reverse primer 5′-GGG CGG GGC ACT TTT TCA CAG-3′ (bases 2702–2681). *Plunc* primers were based on Genbank sequence (NM_172031) forward primer 5′-GGG GCC TGC TTG GAA AAC TGA C (bases 367–388); reverse primer 5′-GTG ACA TCC AAA CCG CTG AGA ATC (bases 802–779).

In situ hybridization was carried out as previously described (21). Briefly, sections were fixed in 4% paraformaldehyde in 0.1 M phosphate buffer (PB), washed in 0.1 M PB, acetylated in 0.25% acetic anhydrate in 0.1 M triethanolamine, and washed again in PB. After dehydration in graded ethanol, radioactive probes were applied to the slides in 70 μL hybridization mixture (0.3 M NaCl, 10 mM Tris-HCL (pH 8), 1 mM EDTA, 0.05% transfer RNA, 10 mM dithiothreitol, 0.02% Ficoll, 0.02% polyvinylpyrrolidone, 0.02% BSA, and 10% dextran sulphate) and hybridized overnight at 58°C. The next day, slides were rinsed in 4× SSC (1× SSC is 0.15 M sodium chloride, 15 mM trisodium citrate pH 7.0), and treated with ribonuclease A (20 μg/μL) at 37°C for 30 min before being washed in decreasing concentrations of SSC with a

final wash in 0.1% SSC at 60°C and dehydration using graded ethanol. Finally, slides were dried and apposed to Kodak Biomax MR film.

After exposure, autoradiographic films were scanned on an Epson scanner and analyzed with Image-Pro PLUS v4.1.0.0 analysis software (Media Cybernetics, Rockville, MD). Integrated optical density was obtained by reference to a ^{14}C microscale. We measured *Dio2*, *Dio3*, *Mct8*, *Hairless*, *Plunc*, and *Sned1* mRNA expression in four sections spanning the ependymal layer of the third ventricle. *Dio3* mRNA expression was also analyzed bilaterally in three sections containing the amygdala, *Sned1* mRNA bilaterally in three sections containing the VMH, *Trh* mRNA expression bilaterally in three sections containing the PVN, and *Pomc*, *Npy*, and *Agrp* mRNA expression measured bilaterally in three sections containing the ARC. Values were averaged for each animal, and the relative mRNA abundance values were calculated by assigning a 100% expression value for the untreated control group (thyroidectomy rat study), *ad lib*–fed group (fasting–refeeding rat study), or LD-exposed hamsters.

Statistical analysis of nonmicroarray data

Data were analyzed by *t*-test, one-way analysis of variance (ANOVA), or two-way repeated measures ANOVA followed by Tukey post hoc, as appropriate. If data were not normally distributed, a one-way ANOVA on ranks (Kruskal–Wallis) combined with Dunn's test was performed. SigmaPlot v11.0 software (Jandel, San Rafael, CA) was used for analysis. The results are presented as mean ± standard error of the mean (SEM), and differences were considered significant at $p < 0.05$.

Results

Food intake, body weight, and body composition

To assess the effect of chemically induced hypothyroidism on energy balance, body weight and food intake were measured daily. Analysis of body weight revealed a significant interaction between treatment and time ($F = 209.048$, $p < 0.001$). Within the MMI-treated groups, weight gain paralleled the control group until day 11 before body weight plateaued before decreasing slightly by day 22. In the control animals, body weight increased significantly throughout the entire study. Body weight was lower in the MMI-treated rats relative to the control group from day 3 of the experiment ($p < 0.05$) and became significantly different from day 11 onwards ($p < 0.001$; Fig. 1A).

Within the control and the MMI-treated groups, food intake (g/100 g body weight) decreased over the course of the experiment (control day 1 vs. day 22: $p < 0.001$; MMI day 1 vs. day 22: $p < 0.001$; Fig. 1B). Food intake (g/100 g body weight) was significantly lower in the MMI-treated groups compared with the control group from day 1 of MMI treatment ($p < 0.009$ at all days), and there was no effect on food intake over the 24 hour period after i.p. administration of T3.

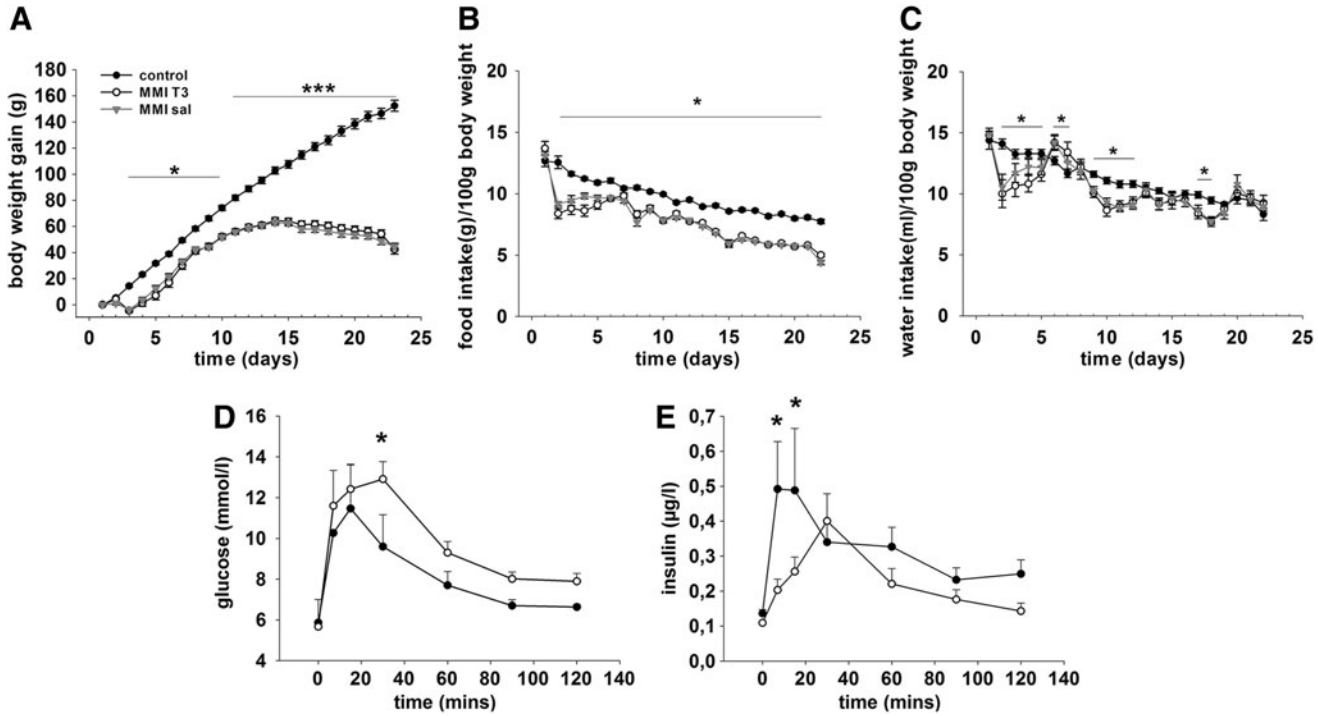

FIG. 1. (**A**) Body weight gain, (**B**) food intake, and (**C**) water intake of Sprague Dawley rats that were either untreated (black circle, control) or rendered hypothyroid by 0.025% methimazole (MMI) in the drinking water with weekly injection of iopanoic acid (100 mg/kg). MMI-T3 rats (white circle) were injected with T3 (25 µg/100 g body weight), and MMI-sal rats (gray triangle) with saline on day 21 of the experiment. Data are presented as mean ± standard error of the mean (SEM). $*p < 0.05$; $***p < 0.001$. (**D**) Serum glucose and (**E**) insulin concentrations during a glucose tolerance test (1 g/kg i.p.) performed on rats that were either untreated (black circles) or rendered hypothyroid over 21 days (white circles). Data are presented as mean ± SEM. $*p < 0.05$.

Water intake (mL/100 body weight) varied on a daily basis in MMI-treated rats compared with control rats on several days during the study (decreased days 2–5, days 9–12, day 17, and day 18, $p < 0.05$; increased days 6 and 7, $p < 0.05$, Fig. 1C). However, average daily water intake over the entire study was not significantly different (MMI: 10.4 mL/100 g body weight vs. control: 11.2 mL/100 g body weight).

Body fat mass was analyzed by magnetic resonance imaging (MRI) showed significantly less fat gain in MMI groups (day 21; fat mass gain MMI rats 6.5 g vs. control rats 11.7 g, $p < 0.001$). Furthermore, lean mass gain was significantly lower in the MMI-treated animals (day 21, lean mass gain MMI rats 37.6 g, control rats 117.5 g, $p < 0.001$).

Serum analysis

To assess the effectiveness of the MMI treatment and T3 injection, T3, T4, and TSH were analyzed in the serum *post mortem* (Table 1). Compared to the control group, *post mortem* serum levels of T3 were reduced by 50% in MMI-treated animals injected with saline ($p < 0.05$). After T3 administration to MMI-treated rats, T3 concentrations were more than 30-fold higher after 24 h compared with control animals ($p < 0.05$). Serum T4 levels were decreased by up to 80% in both MMI-sal and MMI-T3 groups relative to the control group ($p < 0.05$). TSH serum levels were low in control animals and increased 12-fold in the MMI-sal group ($p < 0.05$). In MMI-T3-treated rats, TSH serum concentrations were not different from levels of the control animals.

NEFAs were increased by up to 90% in MMI-treated rats ($p < 0.05$), whereas triglycerides were decreased by 60% in all MMI-treated rats when compared with control rats ($p < 0.05$). T3 injection did not influence NEFA or triglyceride concentrations 24 h after administration (NEFAs $p < 0.05$; tryglicerides $p < 0.05$). Glucose levels were similar in all groups, whereas terminal insulin levels decreased by 50% in both MMI-sal groups compared with controls (Table 1).

To assess whether changes in terminal insulin levels affected the glucose tolerance of MMI-treated rats, we carried out a further study on 16 rats. In these animals, an i.p. glucose tolerance test (i.p. injections of 1 g/kg body weight glucose) was performed on day 20, which revealed impaired glucose clearance (at 30 min after injection, $p = 0.029$; area under the curve 1177.9 ± 61 MMI treatment vs. 976.9 ± 54.4 Con, $p = 0.027$) and decreased insulin secretion (7 min after injection and 15 min after injection, $p = 0.001$ and $p = 0.008$ respectively) in the hypothyroid rats (Fig. 1D and E).

Effects of chemically induced hypothyroidism and T3 administration on the hypothalamic thyroid hormone system

In situ hybridization of components involved in the regulation of hypothalamic thyroid hormone metabolism and transport revealed marked differences between the experimental groups. Relative to controls, *Dio2* expression in tanycytes showed intermediate levels in the control group and was increased by 75% in MMI-sal rats ($p < 0.001$), whereas in the MMI-T3 group, *Dio2* expression, although lower, was not statistically different compared with the control group ($p = 0.06$; Fig. 2A). In the ependymal layer and the amygdala, *Dio3* was weakly expressed in the control and MMI-sal groups, but was significantly upregulated in MMI-T3 rats ($p < 0.05$; Fig. 2B and C). Thyroid hormone transporter *Mct8* mRNA was highly expressed in the ependymal layer of control animals and decreased by 60% in MMI-sal rats ($p < 0.001$). In the MMI-T3 group, *Mct8* mRNA levels were comparable to control levels (Fig. 2D), demonstrating that *Mct8* can be directly regulated by T3. *Trh* mRNA expression in the PVN was low in the control animals and increased 4.5-fold in the MMI-sal group ($p < 0.001$). In MMI-T3 animals, *Trh* mRNA levels were decreased relative to MMI-sal animals by 50% ($p < 0.001$) but were still 150% higher than in the control group ($p = 0.003$, Fig. 2E).

Effects of chemically induced hypothyroidism and T3 injection on hypothalamic systems of energy balance regulation

No differences between the experimental groups were found for orexigenic *Npy* (Fig. 3A) or anorexigenic *Pomc* mRNA expression (Fig. 3C) in the arcuate nucleus, but expression of orexigenic *Agrp* mRNA was significantly decreased by 50% in MMI-sal rats relative to control and MMI-T3 rats ($p < 0.001$; Fig. 3B).

Microarray analysis of hypothalamic RNA from hypothyroid versus hypothyroid-T3-injected Sprague Dawley rats

To screen for novel mechanisms driven by T3 in the brain, mRNA extracted from hypothalamic blocks spanning the

TABLE 1. ANALYSIS OF SERUM METABOLIC MARKERS AND HORMONES IN CONTROL AND CHEMICALLY INDUCED HYPOTHYROID RATS WITH (MMI-T3) OR WITHOUT (MMI-SAL) T3 ADMINISTRATION 24 HOURS BEFORE KILLING

	Control	*MM-T3*	*MMI-sal*	*Control vs. MMI-T3* p-*value*	*Control vs. MMI-sal* p-*value*	*MMI-sal vs. MM-T3* p-*value*
T3 (nmol/L)	0.77 ± 0.06	26.79 ± 1.95	0.38 ± 0.06	< 0.05	< 0.05	< 0.05
T4 (nmol/L)	51.00 ± 7.75	13.38 ± 0.84	11.41 ± 0.79	< 0.05	< 0.05	n.s.
TSH (mE/L)	1.11 ± 0.16	1.15 ± 0.08	12.98 ± 0.89	n.s.	< 0.05	< 0.05
NEFAs (mmol/L)	0.094 ± 0.007	0.181 ± 0.017	0.175 ± 0.016	< 0.05	< 0.05	n.s.
Triglycerides (mmol/L)	1.34 ± 0.09	0.52 ± 0.05	0.53 ± 0.03	< 0.05	< 0.05	n.s.
Glucose (mmol/L)	9.38 ± 0.19	9.69 ± 0.28	9.36 ± 0.32	n.s.	n.s.	n.s.
Insulin (μg/L)	0.32 ± 0.04	0.17 ± 0.01	0.16 ± 0.01	< 0.05	< 0.05	n.s.

MMI, methimazole; T3, triiodothyronine; T4, thyroxine; TSH, thyrotropin; n.s., not significant.

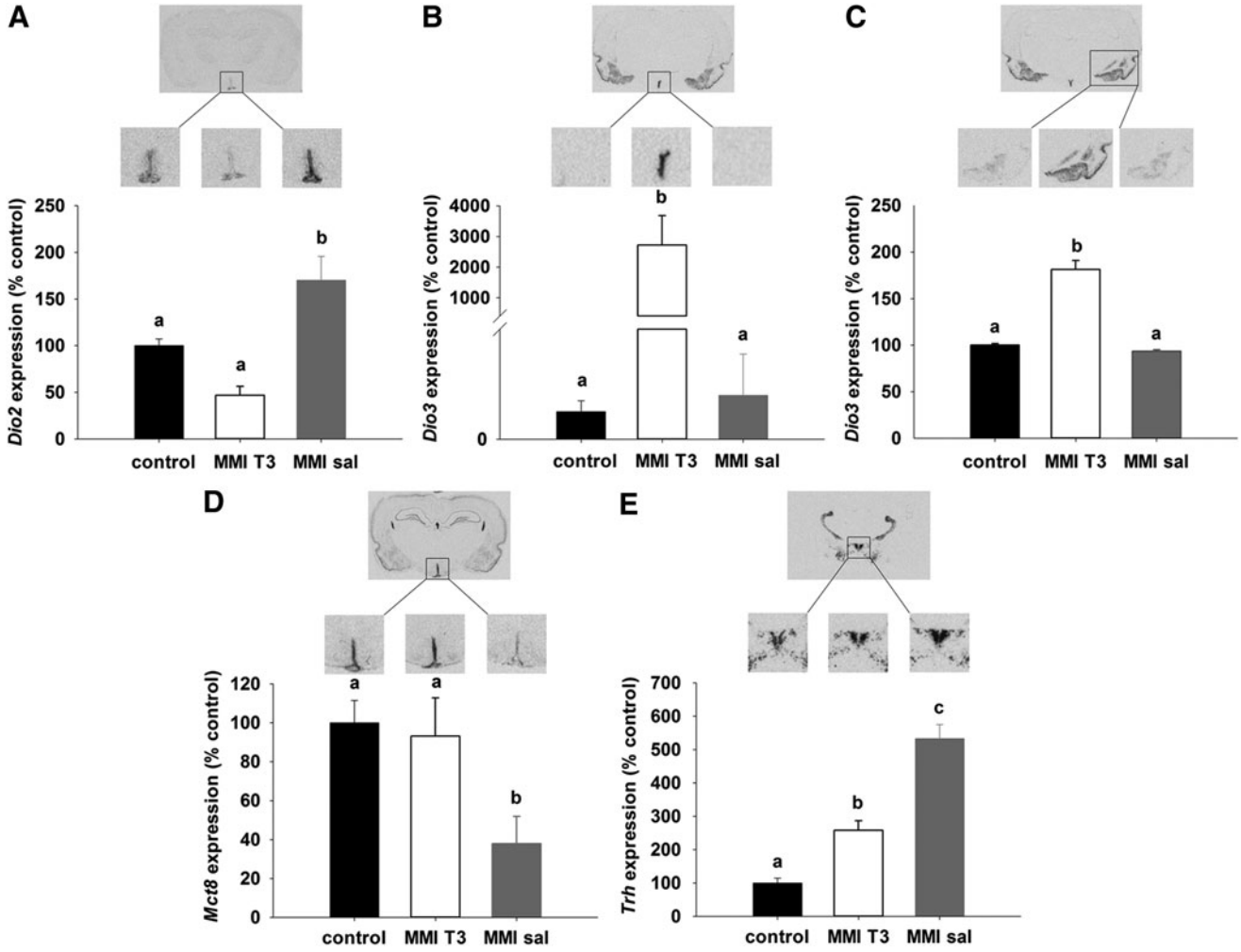

FIG. 2. Autoradiographs and analysis of (**A**) *Dio2*, (**B**) *Dio3*, (**D**) *Mct8*, and (**E**) *Trh* gene expression in the hypothalamus and *Dio3* in the amygdala (**C**) by *in situ* hybridization. Sprague Dawley rats were either untreated (control, $n = 9$, black bars) or rendered hypothyroid over 21 days as in Figure 1 before being injected with T3 (MMI-T3, $n = 8$, white bars) or saline (MMI-sal, $n = 8$, gray bars). Expression was normalized to the control group. Data are presented as mean ± SEM. Bars with different letters are significantly different between treatments.

volume of the arcuate nucleus were analyzed using Agilent whole genome microarrays. This analysis revealed that 85 genes were upregulated by T3 treatment compared with MMI-Sal-treated rats, whereas 25 were downregulated with a greater than 1.3-fold change (at a false discovery rate threshold of 0.25; Tables 2 and 3).

Analysis of expression of differentially expressed genes in the hypothalamus of animal models of body weight regulation

To verify the microarray data, three candidate genes were chosen on the basis of possible involvement in energy balance or neurogenesis, based on either description or preliminary *in situ* hybridization data. The first candidate gene was the insulin responsive element binding protein 1 (*SNED1*) gene, which encodes a transcription factor that may be involved in insulin-regulated gene expression (38–41). *In situ* hybridization revealed that *Sned1* expression in the hypothalamus was restricted to the ependymal layer of the third ventricle and the ventromedial nucleus (VMN). Quantification of the signal in the ependymal layer demonstrated an increase of *Sned1* in MMI-T3 rats relative to control and MMI-sal groups (130% and 160% respectively; $p < 0.001$; Fig. 4A). No regulation of *Sned1* was observed in the ependymal layer of rats that were food deprived for 48 h and then re-fed (Fig. 4B). In the ependymal layer of Siberian hamsters, *Sned1* was 80% higher in LD compared to SD hamsters ($p < 0.001$; Fig. 4C). In the VMN, *Sned1* was increased by T3 administration to hypothyroid rats by 13-fold compared to the euthyroid control group, and it was mostly undetectable in hypothyroid rats treated with saline ($p < 0.001$; Fig. 4D). There was no effect of fasting or re-feeding on *Sned1* mRNA expression, and *Sned1* mRNA expression was not detectable in the VMN of the Siberian hamster (data not shown).

Among the other candidate genes identified were members of the Wnt signaling pathway. These play a role in axon guidance and stem cell proliferation, including *Hairless*, which is expressed in the ependymal layer of the third ventricle and ARC. In both the ARC and ependymal cells,

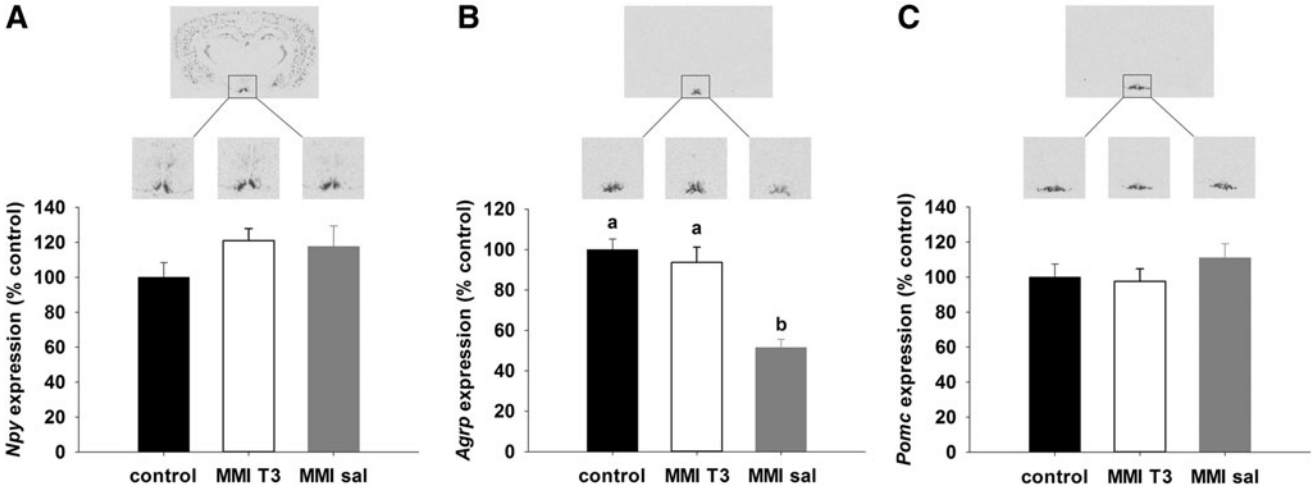

FIG. 3. Representative film images and quantification of (**A**) *Npy*, (**B**) *Agrp*, and (**C**) *Pomc* gene expression in the arcuate nucleus of Sprague Dawley rats by *in situ* hybridization. Animals were either untreated (control, $n = 9$, black bars) or rendered hypothyroid as in Figure 1 over 21 days before being injected with T3 (MMI-T3, $n = 8$, white bars) or saline (MMI-sal, $n = 8$, gray bars). Expression was normalized to the control group. Data are presented as mean ± SEM. Bars with different letters are significantly different between treatments.

Hairless mRNA was increased by sixfold in MMI-T3 animals compared with control ($p < 0.05$) and was undetectable in the MMI-Sal group (Fig. 5A). *Hairless* mRNA expression in the ependymal layer was not affected by fasting and refeeding in Sprague Dawley rats (Fig. 5B). In Siberian hamsters, *Hairless* mRNA expression was restricted to the ependymal layer, where it was 60% higher in the LD compared to the SD state ($p < 0.001$; Fig. 5C).

Expression of the *Plunc* mRNA in the hypothalamus was restricted to the ependymal walls of the third ventricle and the adjacent ARC in rats. *Plunc* mRNA levels were increased by 4.5-fold after injection of T3 in the MMI-T3 group relative to control ($p < 0.05$) and MMI-sal-treated rats ($p < 0.05$; Fig. 5D) animals. Relative to *ad libitum* fed rats, fasting decreased *Plunc* expression by 70% ($p < 0.05$), and mRNA levels remained low (decreased by 80%) even after 24 h re-feeding ($p < 0.05$; Fig. 5E). No *Plunc* expression was detected in the hypothalamus of Siberian hamsters (data not shown).

Discussion

Many studies have shown that circulating thyroid hormones are involved in the regulation of energy balance and body weight in mammals (7–9). Over the past decade, evidence has arisen that thyroid hormones not only act in the periphery but may also act in the brain in areas such as the hypothalamus to regulate food intake and energy expenditure (10,28). Although T3 is known to have significant effects on brain development, little is known about its role in the adult brain, particularly within the hypothalamic nuclei where many of the homeostatic control neurons regulating reproduction, food intake, energy expenditure, glucose homeostasis, and thermoregulation are located. Using microarray analysis of gene expression comparing hypothyroid and hyperthyroid states, we have identified potential targets of thyroid hormone action in the adult rat hypothalamus.

MMI decreased food intake and body weight and altered body composition of adult Sprague Dawley rats

Over the course of 22 days, MMI treatment was effective at inducing hypothyroidism, resulting in a 50% decrease in circulating T3, an approximately 80% decrease in circulating T4 concentrations, and substantially elevated circulating TSH levels. Intraperitoneal administration of T3, a model in which elevated T3 levels were measurable 24 hours after injection, had no effect on circulating T4 but corrected circulating TSH concentrations, as anticipated for the regulatory feedback mechanism of thyroid hormone homeostasis (7). Food and water intake (g/100 g and mL/100 g body weight respectively) showed a decline over time, but only food intake was significantly different throughout the treatment, whereas water intake was variable and overall not significantly different by the end of the treatment period. Body weight was profoundly affected by hypothyroidism induced by MMI, consistent with other studies on hypothyroidism in rats (12,42,43). Reduced body weight gain of MMI-treated rats was accompanied by reductions in both lean and fat tissue.

Circulating NEFAs were increased, while triglycerides were decreased, indicative of utilization of lipid as energy substrate. Nonfasted glucose levels at termination were not different between control and treatments, but basal insulin levels were reduced in MMI-treated rats compared with controls, and were not restored within 24 hours after T3 administration.

The reduction in circulating insulin indicates a possible perturbation of glucose homeostasis, and an i.p glucose tolerance test showed impaired glucose clearance. Insulin secretion was also impaired, with the primary effect appearing to be exerted on the first-phase insulin secretion, which occurs within the first 20 min following glucose administration, whereas the secondary phase of insulin secretion, which occurs beyond 20 minutes after glucose administration, was largely unaffected; these responses are features of a diabetic state (44).

Table 2. Genes Upregulated in the Hypothalamus by T3 Administration to Hypothyroid Rats

Name	*GeneName*	*Description*	*Average intensity*	*Fold change*	p-*Value*
XM_217299	Gup1_predicted	PREDICTED: Rattus norvegicus Gup1, glycerol uptake/transporter homolog (yeast) (predicted) (Gup1_predicted), mRNA	11.88249	5.268017	8.97E-07
NM_053562	Rpe65	Rattus norvegicus retinal pigment epithelium 65 (Rpe65), mRNA	9.118793	4.0298	8.64E-05
NM_172031	Plunc	Rattus norvegicus palate, lung, and nasal epithelium carcinoma associated (Plunc), mRNA	9.414428	3.475227	5.94E-06
NM_017210	Dio3	Rattus norvegicus deiodinase, iodothyronine, type III (Dio3), mRNA	10.41265	3.199039	0.001511
TC551251	TC551251	Unknown	9.611597	2.928708	4.30E-05
XM_213226	XM_213226	Rattus norvegicus similar to RIKEN cDNA 2810417J12 gene (LOC287103), mRNA	12.88989	2.872941	2.43E-06
NM_019361	Arc	Rattus norvegicus activity regulated cytoskeletal-associated protein (Arc), mRNA	10.23297	2.847995	5.85E-05
NM_057211	Klf9	Rattus norvegicus Kruppel-like factor 9 (Klf9), mRNA	11.96643	2.808296	1.65E-05
NM_001009623	Tnfsf13	Rattus norvegicus tumor necrosis factor (ligand) superfamily, member 13 (Tnfsf13), mRNA	9.461335	2.732492	5.83E-06
XM_001053566	Gli2_predicted	PREDICTED: Rattus norvegicus GLI-Kruppel family member GLI2 (predicted) (Gli2_predicted), mRNA	9.755351	2.712706	0.000101
AW144489	AW144489	AW144489 EST294866 Normalized rat placenta, Bento Soares Rattus sp. cDNA clone RGIAJ29 5′ end, mRNA sequence	12.44283	2.693911	1.40E-05
TC541217	TC541217	Unknown	10.58327	2.650032	2.04E-05
NM_130739	Acsl6	Rattus norvegicus acyl-CoA synthetase long-chain family member 6 (Acsl6), mRNA	12.33923	2.550024	7.09E-06
NM_001025773	LOC500590	Rattus norvegicus similar to T-cell antigen 4-1BB precursor - mouse (LOC500590), mRNA	7.500685	2.434286	8.60E-05
XM_001057993	LOC680611	PREDICTED: Rattus norvegicus similar to B-cell leukemia/ lymphoma 3 (LOC680611), mRNA	9.147575	2.377847	7.09E-06
NM_012737	Apoa4	Rattus norvegicus apolipoprotein A-IV (Apoa4), mRNA	7.867637	2.316784	0.001923
XM_001060674	LOC681186	PREDICTED: Rattus norvegicus hypothetical protein LOC681186 (LOC681186), mRNA	8.601423	2.244997	0.00054
XM_341550	Akr1cl1_predicted	PREDICTED: Rattus norvegicus aldo-keto reductase family 1, member C-like 1 (predicted) (Akr1cl1_predicted), mRNA	10.96448	2.22358	1.46E-05
TC526109	TC526109	Unknown	11.19203	2.198008	0.000212
NM_001013053	Defcr4	Rattus norvegicus defensin related cryptdin 4 (Defcr4), mRNA	7.060291	2.134	0.000424
NM_022407	Aldh1a1	Rattus norvegicus aldehyde dehydrogenase family 1, member A1 (Aldh1a1), mRNA	9.158333	2.131812	0.00063
NM_031766	Cpz	Rattus norvegicus carboxypeptidase Z (Cpz), mRNA	8.963887	2.109028	5.83E-05
XM_001063973	Trp53inp2	PREDICTED: Rattus norvegicus tumor protein p53 inducible nuclear protein 2 (Trp53inp2), mRNA	10.71086	2.100622	1.82E-05

(*continued*)

TABLE 2. (CONTINUED)

Name	*GeneName*	*Description*	*Average intensity*	*Fold change*	p-*Value*
XM_343919	Jmjd3_predicted	PREDICTED: Rattus norvegicus jumonji domain containing 3 (predicted) (Jmjd3_predicted), mRNA	10.13486	2.000512	0.003565
TC528506	TC528506	Unknown	7.655836	1.989516	0.00014
DV729077	DV729077	RVL21838 Wackym-Soares normalized rat vestibular cDNA library Rattus norvegicus cDNA 5′, mRNA sequence	10.19553	1.961121	0.00014
NM_133569	Angptl2	Rattus norvegicus angiopoietin-like 2 (Angptl2), mRNA	8.250958	1.86886	0.000625
NM_017061	Lox	Rattus norvegicus lysyl oxidase (Lox), mRNA	9.016704	1.86698	4.21E-05
NM_133581	Wfdc1	Rattus norvegicus WAP four-disulfide core domain 1 (Wfdc1), mRNA	10.9154	1.866866	0.000266
NM_001012123	C1qtnf5	Rattus norvegicus C1q and tumor necrosis factor related protein 5 (C1qtnf5), mRNA	10.08157	1.864286	0.000185
NM_024364	hr	Rattus norvegicus hairless homolog (mouse) (hr), mRNA	7.760339	1.85893	3.68E-05
XM_227657	Bcar3_predicted	PREDICTED: Rattus norvegicus breast cancer anti-estrogen resistance 3 (predicted) (Bcar3_predicted), mRNA	7.512116	1.807788	6.84E-05
NM_017189	Asgr2	Rattus norvegicus asialoglycoprotein receptor 2 (Asgr2), mRNA	7.497761	1.798794	0.000404
NM_212528	Col11a2_mapped	Rattus norvegicus procollagen, type XI, alpha 2 (mapped) (Col11a2_mapped), mRNA	12.53966	1.792179	0.000247
NM_001014068	Gloxd1	Rattus norvegicus glyoxalase domain containing 1 (Gloxd1), mRNA	8.359035	1.790356	0.000437
XM_001069205	LOC684158	PREDICTED: Rattus norvegicus similar to chromosome 1 open reading frame 36 (LOC684158), mRNA	7.605397	1.779589	0.000149
XM_001078245	LOC691431	PREDICTED: Rattus norvegicus similar to mitochondrial carrier protein MGC4399 (LOC691431), mRNA	11.1205	1.758199	0.00064
XM_213343	Dhrs7c_predicted	PREDICTED: Rattus norvegicus dehydrogenase/reductase (SDR family) member 7C (predicted) (Dhrs7c_predicted), mRNA	7.714002	1.740514	5.31E-05
TC543145	TC543145	Unknown	8.12121	1.706816	0.000218
TC539072	TC539072	Unknown	9.313955	1.700501	0.000267
NM_013060	Id2	Rattus norvegicus inhibitor of DNA binding 2 (Id2), mRNA	10.90673	1.697194	0.000321
TC550302	TC550302	Unknown	9.401051	1.675177	6.90E-05
AW914057	AW914057	AW914057 EST294835 Rat gene index, normalized rat, norvegicus, Bento Soares Rattus norvegicus cDNA clone RGIZB86 5′ end, mRNA sequence	7.748432	1.659375	0.000227
NM_001014843	Faim3	Rattus norvegicus Fas apoptotic inhibitory molecule (Faim3), mRNA	8.360821	1.648237	1.00E-04
NM_013156	Ctsl	Rattus norvegicus cathepsin L (Ctsl), mRNA	14.49999	1.645066	0.000138
NM_133621	Hod	Rattus norvegicus homeobox only domain (Hod), mRNA	12.63979	1.636147	0.000138
NM_013161	Pnlip	Rattus norvegicus pancreatic lipase (Pnlip), mRNA	8.776656	1.628099	0.000153

(*continued*)

TABLE 2. (CONTINUED)

Name	*GeneName*	*Description*	*Average intensity*	*Fold change*	p-*Value*
AY035551	AY035551	Rattus norvegicus brain Ntab mRNA sequence	13.02346	1.627153	0.000234
NM_012571	Got1	Rattus norvegicus glutamate oxaloacetate transaminase 1 (Got1), mRNA	13.66552	1.613406	0.000306
AW143634	AW143634	AW143634 EST293930 Normalized rat embryo, Bento Soares Rattus sp. cDNA clone RGIBX04 5′ end, mRNA sequence	9.049826	1.611212	0.000184
NM_022955	Egfl3	Rattus norvegicus EGF-like-domain, multiple 3 (Egfl3), mRNA	8.614611	1.610819	0.000384
BF545795	BF545795	BF545795 UI-R-BT0-qc-d-07-0-UI.r1 UI-R-BT0 Rattus norvegicus cDNA clone UI-R-BT0-qc-d-07-0-UI 5′, mRNA sequence	8.808667	1.601778	0.000269
TC539984	TC539984	Unknown	12.82382	1.600383	0.000139
XM_576205	RGD1562092_predicted	PREDICTED: Rattus norvegicus similar to regulatory factor×4 variant (predicted) (RGD1562092_predicted), mRNA	10.53032	1.596132	0.000173
NM_031612	Apln	Rattus norvegicus apelin, AGTRL1 ligand (Apln), mRNA	13.2519	1.595306	9.70E-05
XM_215659	Rhoc_predicted	PREDICTED: Rattus norvegicus ras homolog gene family, member C (predicted) (Rhoc_predicted), mRNA	9.247711	1.587147	0.00035
AF439716	Sned1	Rattus norvegicus isolate No:6 insulin responsive sequence DNA binding protein-1 mRNA, partial cds.	8.328124	1.586158	0.000625
XM_216484	RGD1305274_predicted	PREDICTED: Rattus norvegicus similar to RIKEN cDNA 2010305A19 (predicted) (RGD1305274_predicted), mRNA	9.306172	1.581836	9.97E-05
XM_216399	Col15a1	PREDICTED: Rattus norvegicus procollagen, type XV (Col15a1), mRNA	7.669346	1.575705	0.000274
TC520453	TC520453	Unknown	9.046111	1.567977	0.00065
NM_001012034	Art3	Rattus norvegicus ADP-ribosyltransferase 3 (Art3), mRNA	8.22811	1.558209	0.00018
NM_031135	Klf10	Rattus norvegicus Kruppel-like factor 10 (Klf10), mRNA	8.0567	1.554988	0.000509
XM_001056128	Gli1	PREDICTED: Rattus norvegicus GLI-Kruppel family member GLI1 (Gli1), mRNA	10.25812	1.553615	0.000159
TC539426	TC539426	O41021 (O41021) A312aR protein, partial (19%)	8.040854	1.54991	0.000389
NM_053445	Fads1	Rattus norvegicus fatty acid desaturase 1 (Fads1), mRNA	10.57416	1.549564	0.00047
XM_001077248	Hcn2	PREDICTED: Rattus norvegicus hyperpolarization activated cyclic nucleotide-gated potassium channel 2 (Hcn2), mRNA	13.79632	1.548731	0.00019
AW915407	AW915407	AW915407 EST346711 Normalized rat embryo, Bento Soares Rattus sp. cDNA clone RGICV10 5′ end, mRNA sequence	9.642406	1.541304	0.000289
A_44_P889730	A_44_P889730	Unknown	7.868883	1.535946	0.000332
XM_342915	RGD1308876_predicted	PREDICTED: Rattus norvegicus similar to 2610027C15Rik protein (predicted) (RGD1308876_predicted), mRNA	11.33458	1.528331	0.000512

(*continued*)

TABLE 2. (CONTINUED)

Name	*GeneName*	*Description*	*Average intensity*	*Fold change*	p-*Value*
XM_214510	RGD1308977_predicted	PREDICTED: Rattus norvegicus similar to RIKEN cDNA 1110017I16 (predicted) (RGD1308977_predicted), mRNA	8.749831	1.527016	0.00018
BF559362	BF559362	BF559362 UI-R-E1-fc-a-10-0-UI.r1 UI-R-E1 Rattus norvegicus cDNA clone UI-R-E1-fc-a-10-0-UI 5′, mRNA sequence	8.883881	1.516901	0.000261
TC552370	TC552370	Q6MG84 (Q6MG84) NG3 protein, partial (32%)	9.589327	1.511642	0.000508
NM_001004274	Igfbp4	Rattus norvegicus insulin-like growth factor binding protein 4 (Igfbp4), mRNA	9.063962	1.503451	0.000557
XM_341391	Plac9_predicted	PREDICTED: Rattus norvegicus placenta-specific 9 (predicted) (Plac9_predicted), mRNA	9.655327	1.503303	0.000226
NM_019282	Grem1	Rattus norvegicus gremlin 1 homolog, cysteine knot superfamily (Xenopus laevis) (Grem1), mRNA	8.721548	1.50303	0.000204
CF106882	CF106882	Shultzomica00133 Rat lung airway and parenchyma cDNA libraries Rattus norvegicus cDNA clone Contig2296 5′, mRNA sequence	10.15976	1.492289	0.000222
NM_001030054	LOC595134	Rattus norvegicus hypothetical protein LOC595134 (LOC595134), mRNA	10.84267	1.484176	0.000368
NM_012503	Asgr1	Rattus norvegicus asialoglycoprotein receptor 1 (Asgr1), mRNA	8.382358	1.475312	0.00061
XM_573694	Nid2	PREDICTED: Rattus norvegicus nidogen 2 (Nid2), mRNA	8.302673	1.455202	0.000335
NM_012800	P2ry1	Rattus norvegicus purinergic receptor P2Y, G-protein coupled 1 (P2ry1), mRNA	7.548232	1.454061	0.000276
NM_133568	Rasd2	Rattus norvegicus RASD family, member 2 (Rasd2), mRNA	8.234835	1.432896	0.000635
XM_218935	Kctd14_predicted	PREDICTED: Rattus norvegicus potassium channel tetramerization domain containing 14 (predicted) (Kctd14_predicted), mRNA	7.633445	1.411129	0.000517
A_44_P597956	A_44_P597956	Unknown	9.15148	1.405745	0.000612
XM_226016	Pura_predicted	PREDICTED: Rattus norvegicus purine rich element binding protein A (predicted) (Pura_predicted), mRNA	14.47377	1.39965	0.000649
NM_022858	Foxq1	Rattus norvegicus forkhead box Q1 (Foxq1), mRNA	7.538355	1.357339	0.000608

MMI treatment and T3 injections affect gene expression in the hypothalamus

The thyroid hormone system in the hypothalamus was affected by the thyroid hormone status of MMI-treated animals, indicative of low central thyroid hormone levels. *Dio2* mRNA expression in the tanycytes of the third ventricle was increased in MMI-treated rats by the lower circulating thyroid hormone levels, an effect that can be observed with propylthiouracil (PTU) administration (22). The MMI-induced increase in *Dio2* mRNA expression was reversed by T3 administration within 24 hours. The most parsimonious explanation for increased *Dio2* mRNA expression is a compensatory response endeavoring to maintain T3 in the hypothalamus and other brain regions at levels required for optimal function. Reduced thyroid hormone levels induced a compensatory response of *Trh* mRNA expression in the PVN, which was significantly reduced by T3 administration within 24 hours. However, *Trh* mRNA levels were still significantly elevated relative to euthyroid control rats. One possible reason for this delay in the adjustment of *Trh* mRNA levels is an insufficient exposure of PVN neurons to circulating T3. This may have arisen because of a possible reduction of T3/T4 transport due to iopanoic acid. Iopanoic acid was used to enhance the state of hypothyroidism by inhibiting deiodinase enzymes. However, it is known that iopanoic acid reduces T4 transport by Oatp1c1, a high affinity T4 transporter (45,46). Whether there is any impact on transport by other primary or secondary T3/T4 transporters is unknown (47). However, *Dio3* mRNA expression in the amygdala was

Table 3. Genes Downregulated in the Hypothalamus by T3 Administration to Hypothyroid Rats

Name	*GeneName*	*Description*	*Average intensity*	*Fold change*	p-*Value*
NM_031655	Lxn	Rattus norvegicus latexin (Lxn), mRNA	12.66201	−1.35033	0.000648
XM_001057696	LOC680551	PREDICTED: Rattus norvegicus similar to Apolipoprotein C-IV precursor (Apo-CIV) (ApoC-IV) (Apolipoprotein C2-linked) (ACL) (LOC680551), mRNA	7.883503	−1.38783	0.000567
BG378227	BG378227	BG378227 UI-R-CV1-bvp-e-08-0-UI.s1 UI-R-CV1 Rattus norvegicus cDNA clone UI-R-CV1-bvp-e-08-0-UI 3′, mRNA sequence	8.967155	−1.41934	0.000535
NM_001007611	RGD1359691	Rattus norvegicus hypothetical LOC287534 (RGD1359691), mRNA	10.1962	−1.43904	0.000486
XM_001072931	Rgc32	PREDICTED: Rattus norvegicus response gene to complement 32 (Rgc32), mRNA	12.76325	−1.4407	0.000328
XM_215897	Acss1_predicted	PREDICTED: Rattus norvegicus acyl-CoA synthetase short-chain family member 1 (predicted) (Acss1_predicted), mRNA	10.24754	−1.44698	0.000452
NM_017080	Hsd11b1	Rattus norvegicus hydroxysteroid 11-beta dehydrogenase 1 (Hsd11b1), mRNA	11.85208	−1.45705	0.000281
XM_228918	Egfl6	PREDICTED: Rattus norvegicus EGF-like-domain, multiple 6 (Egfl6), mRNA	8.049509	−1.45987	0.00052
AJ003232	AJ003232	RNAJ3232 Rattus norvegicus mRNA for MHC class II RT1-D beta1 chain haplotype k	8.027006	−1.46109	0.000294
NM_139185	Gng8	Rattus norvegicus guanine nucleotide binding protein (G protein), gamma 8 subunit (Gng8), mRNA	11.97161	−1.46169	0.000535
XM_214671	XM_214671	Rattus norvegicus hypothetical LOC291982 (LOC291982), mRNA	9.387132	−1.4865	0.000345
AW915522	AW915522	AW915522 EST346826 Normalized rat embryo, Bento Soares Rattus sp. cDNA clone RGICW33 5′ end, mRNA sequence	10.68714	−1.49131	0.000305
NM_031853	Dbi	Rattus norvegicus diazepam binding inhibitor (Dbi), mRNA	15.08979	−1.54028	0.000191
NM_019195	Cd47	Rattus norvegicus CD47 antigen (Rh-related antigen, integrin-associated signal transducer) (Cd47), mRNA	11.3667	−1.5486	0.000156
NM_138530	Mawbp	Rattus norvegicus MAWD binding protein (Mawbp), mRNA	12.24495	−1.58734	0.00021
XM_237195	LOC301444	PREDICTED: Rattus norvegicus pseudogene for diazepam binding inhibitor 1 (LOC301444), mRNA	9.247721	−1.59304	0.000479
TC525753	TC525753	Unknown	7.984411	−1.60262	0.00012
NM_012493	Afp	Rattus norvegicus alpha-fetoprotein (Afp), mRNA	8.675151	−1.61028	0.000542
NM_144750	LOC246266	Rattus norvegicus lysophospholipase (LOC246266), mRNA	9.523682	−1.72725	0.000221

(*continued*)

TABLE 3. (CONTINUED)

Name	*GeneName*	*Description*	*Average intensity*	*Fold change*	p-*Value*
XM_341702	RGD1309651_predicted	PREDICTED: Rattus norvegicus similar to 1190005I06Rik protein (predicted) (RGD1309651_predicted), mRNA	8.892309	−1.74107	0.000133
NM_134326	Alb	Rattus norvegicus albumin (Alb), mRNA	8.237368	−1.87847	0.00036
TC550174	TC550174	Unknown	7.24582	−1.91585	7.30E-05
XM_001065258	LOC683288	PREDICTED: Rattus norvegicus similar to Charged multivesicular body protein 4b (Chromatin-modifying protein 4b) (CHMP4b) (LOC683288), mRNA	11.71853	−2.06669	0.008379
NM_173123	Cyp4f4	Rattus norvegicus cytochrome P450, family 4, subfamily f, polypeptide 4 (Cyp4f4), mRNA	11.15458	−2.07395	0.00184
XM_001057122	LOC681501	PREDICTED: Rattus norvegicus similar to potassium voltage-gated channel, Isk-related family, member 1-like (LOC681501), mRNA	10.65445	−2.21831	3.61E-05

elevated in response to exogenous T3, indicating a widespread penetration of T3 in the brain following administration. Another possible explanation is that *Dio2* mRNA expression, which was lower (but not to significance), and the high levels of *Dio3* mRNA expression in ependymal cells lead to a localized depletion of T3 at the PVN in a hardwired feedback loop between tanycytes and PVN neurons (48). This response, however, serves to illustrate that not all changes in gene expression may have been detected by our approach, and other genes with similar delays in responsiveness to T3 administration may have gone undetected. *Dio3* mRNA expression in the ventricular ependymal cells and amygdala was low in euthyroid and MMI-treated rats, but highly elevated in response to T3 administration, consistent with the known activation by T3 (19). Expression of the thyroid hormone transporter *Mct8* in the ventricular ependymal cells was decreased, but like *Dio2*, *Mct8* mRNA expression was reversed within 24 hours following T3 administration. These data demonstrate for the first time that T3 regulates the expression of the MCT8 transporter in ependymal cells. This is contrary to the increase observed in the hippocampus of postnatal rat pups in response to T3 depletion by MMI and PTU (49). This also contrasts with the photoperiodic regulation of *Mct8* mRNA in the ependymal layer of the third ventricle of the seasonal Siberian hamster where *Mct8* mRNA expression increased in the short photoperiod when hypothalamic levels of T3 are decreased (21).

The profound effect of thyroid hormone on body weight and food intake raises the question of whether thyroid hormone levels directly regulate genes that are involved in energy balance. Here, we investigated the expression of principal orexigenic and anorexigenic genes in the arcuate nucleus (ARC); POMC mediates an anorexigenic effect and increased energy expenditure (50–52), while in contrast NPY-AgRP co-expressing neurons are located in the medial population of ARC neurons and mediate an orexigenic effect and decrease energy expenditure (53–55).

Previously Diano *et al*. (22) have shown that *Dio2* and hypothalamic T3 levels increased by fasting and are involved in activating *Npy* mRNA gene expression involving a mechanism that requires mitochondrial UCP2. In our study, no effect of MMI treatment was observed on basal levels of *Npy* expression. This is consistent with the aforementioned study where *Npy* mRNA was unchanged in a *Dio2* knockout mouse (22). No difference in *Pomc* mRNA expression was observed, suggesting that the anorexigenic drive in the hypothalamus may be unchanged. MMI treatment did, however, result in decreased *Agrp* mRNA expression, which was reversed by T3 injection within 24 hours. AgRP acts as an antagonist of the melanocortin MC4 and MC3 receptors and, when administered i.c.v. or overexpressed, it increases food intake leading to obesity (54–56), while selective ablation in the adult mouse brain confers inappetence (57). Therefore downregulation of *Agrp* mRNA expression in our experiments, together with unchanged *Pomc* mRNA expression, could contribute to the body weight phenotype and the reduction observed in food intake of the MMI-treated rats. These are the first data to show a direct effect of T3 on *Agrp* mRNA expression in a rodent model, and they are consistent with a stimulatory effect of T3 on *Agrp* expression observed in chickens (58). T3 regulation of *Agrp* has also been inferred in a reduced growth response to SD photoperiod in F344 rats (59). Thus, the reduction in *Agrp* mRNA and discoordinated regulation relative to *Npy* mRNA expression in the hypothyroid rat parallels the reduced *Agrp* mRNA expression seen in SD photoperiod exposed F344 rat. Consequently, it is possible that a reduction in the drive of the growth hormone axis may be involved in the context of hypothyroidism leading to reduced lean and fat mass.

Genes regulated by thyroid hormone in the adult brain

To screen for novel mechanisms in the brain involving by T3, we analyzed gene expression of hypothalamic tissue

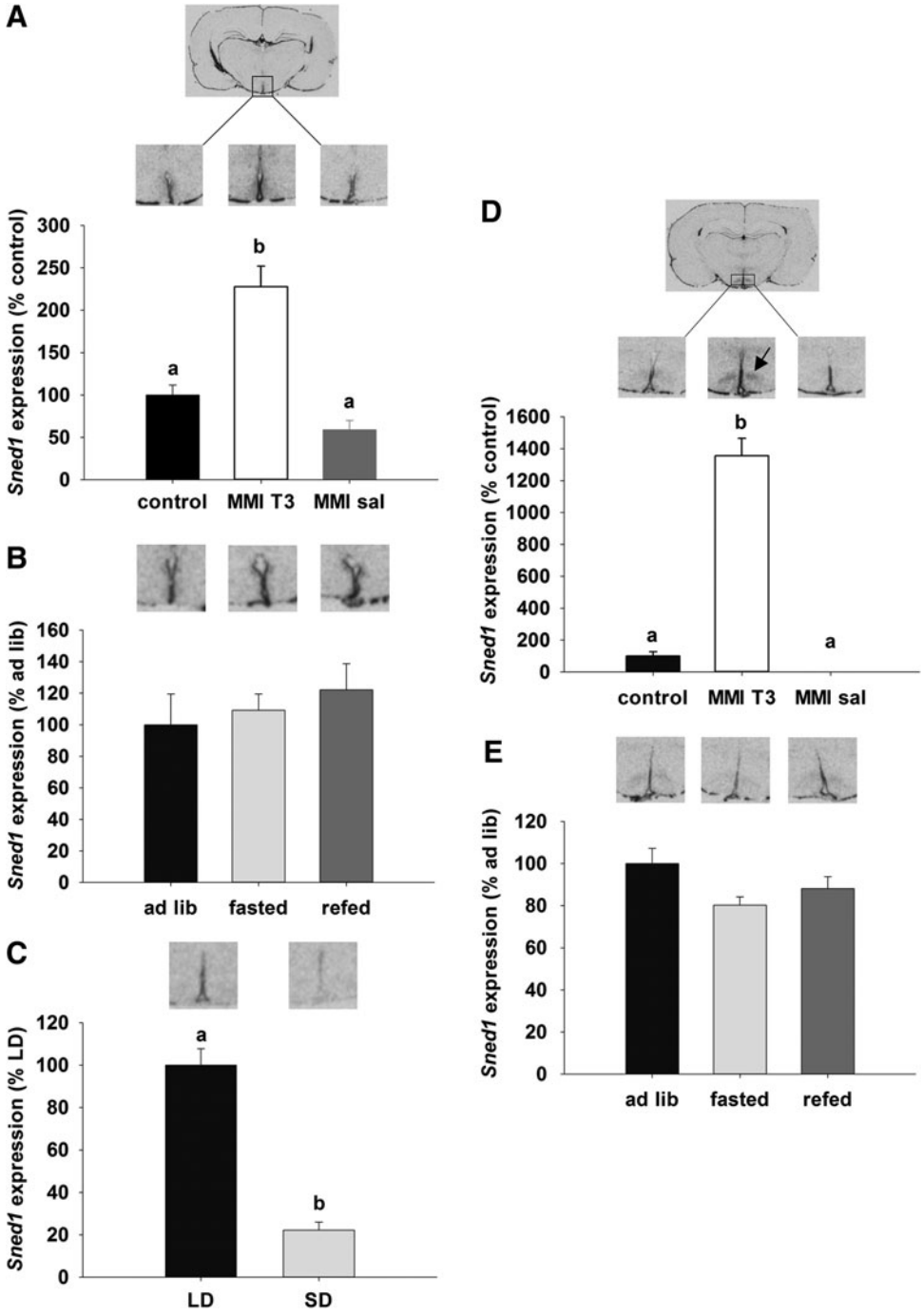

FIG. 4. Autoradiographs and quantification of *Sned1* gene expression by *in situ* hybridization. Gene expression of *Sned 1* was analyzed in the ependymal layer of the third ventricle (**A**) and the VMN (**D**) in Sprague Dawley rats that were untreated (black bar, control, $n=9$) and compared to animals rendered hypothyroid over 21 days as in Figure 1, before being injected with T3 (MMI-T3, $n=8$, white bars) or saline (MMI-sal, $n=8$, gray bars). Expression was normalized to the control group. (**B**) and (**E**) show representative sections and analysis of *Sned1*, in the ependymal layer and VMN respectively of untreated rats that were fed *ad libitum* (black bar, ad lib, $n=8$), fasted for 48 hours (light gray bar, fasted, $n=8$) or fasted for 48 hours and then re-fed for 24 hours (dark gray bar, re-fed, $n=8$). Expression was normalized to *ad libitum* fed animals. (**C**) *Sned1* expression was analyzed in the ependymal layer of Siberian hamsters that were kept in long days (16:8 light:dark, black bar, LD, $n=6$) or short days for 14 weeks (8:16 light:dark, light gray bar, SD, $n=7$). No *Sned 1* expression was present in the VMH of Siberian hamsters. Data were normalized to LD hamsters. Data are presented as mean ± SEM. Bars with different letters are significantly different between treatments. Arrow in (**D**) indicates the VMN.

using Agilent whole genome microarrays. This approach yielded 85 genes that were upregulated and 25 genes that were downregulated by T3 administration to hypothyroid rats. With the exception of *Dio3*, we noted that gene expression changes for *Dio2*, *Mct8*, *Trh*, and *Agrp* were not observed on the array. The reason for this is unclear, and there may be a number of explanations such as T3 replacement does not necessarily substitute for T3 converted from T4 locally within cells, which in our experiments was not restored after T3 administration (60), or that the microarray approach was only sufficiently sensitive to detect changes in the expression of genes with larger differences between the hypothyroid and hyperthyroid states, or that tissues were not taken at an optimal time relative to T3 administration. Nevertheless, several candidate genes, such as those involved in insulin signaling and neurogenesis, were chosen for further investigation based on description, preliminary *in situ* hybridization data, and recent developments on the potential regulation of tanycytes in hypothalamic regulation of food intake.

Sned1

Sned1 encodes an insulin responsive transcription factor, which activates insulin responsive genes downstream of the PI3K-AKT pathway. *In vivo* overexpression of *Sned1* in

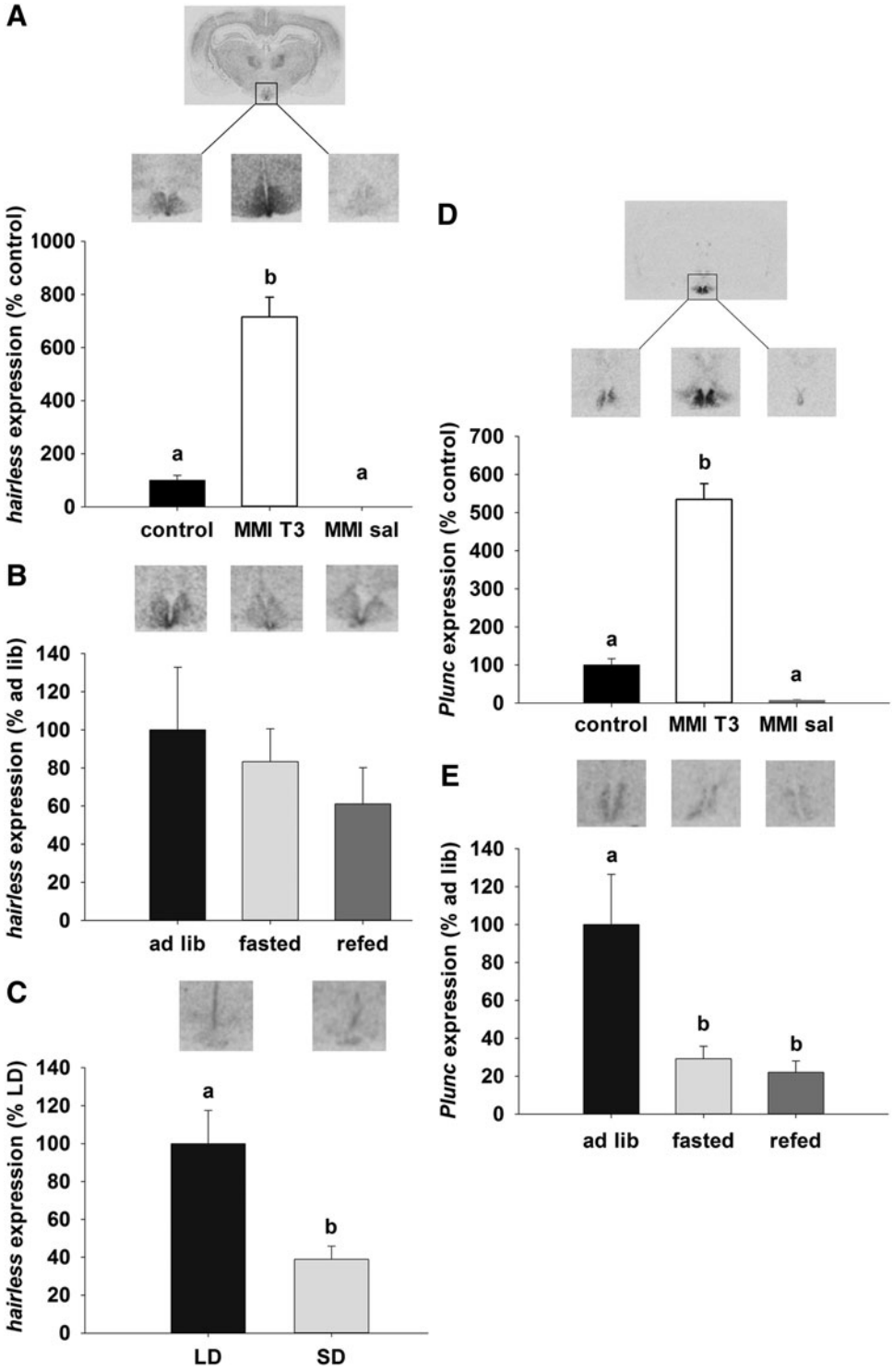

FIG. 5. Representative sections and analysis of (**A**) *Hairless* and (**D**) *Plunc* mRNA expression in the ependymal layer and ARC of Sprague Dawley rats that were untreated (black bar, control, $n = 9$) and compared with animals rendered hypothyroid over 21 days as in Figure 1, before being injected with T3 (MMI-T3, $n = 8$, white bars) or saline (MMI-sal, $n = 8$, gray bars). Expression was normalized to the control group. (**B**) and (**E**) show representative sections and analysis of *Hairless* and *Plunc* mRNA respectively in the ependymal layer of untreated rats that were fed *ad libitum* (black bar, ad lib, $n = 8$), fasted for 48 hours (light gray bar, fasted, $n = 8$) or fasted for 48 hours and then re-fed for 24 hours (dark gray bar, re-fed, $n = 8$). (**C**) *Hairless* expression was analyzed in the ependymal layer of Siberian hamsters that were kept in LD (16:8 light:dark, black bar) or SD for 14 weeks (8:16 light:-dark, light gray bar). No *Plunc* expression was present in the ependymal layer of Siberian hamsters. Data were normalized to LD hamsters. Data are presented as mean ± SEM. Bars with different letters are significantly different.

peripheral tissues can ameliorate hyperglycemia in diabetes or reproduce diabetes, depending on the tissue in which overexpression is engineered (38–41). In accordance with the microarray analysis, *in situ* hybridization revealed an increase of *Sned1* after T3 injection in thyroidectomized rats in the ependymal layer. These cells in the ependymal layer will include the specialized glial cells known as tanycytes. In addition to a presence in the ependymal layer, *Sned1* is also expressed the ventromedial nucleus where it is also increased by T3 administration. This is the first time that the localization of *Sned1* has been described in the brain, and it is interesting to note that the identified areas of the hypothalamus are responsive to insulin or involved in glucose sensing (61,62). This finding may have important implications for the mechanism of glucose sensing and implications for thyroid hormone involvement in glucose homeostasis.

In the Siberian hamster, a model of long-term photoperiodic body weight regulation, *Sned1* was expressed in the

ependymal layer and found to be higher in LD compared to SD hamsters, when hypothalamic T3 levels are elevated (20), but it was undetectable in the VMN of this species, possibly indicating a species difference in this region. Food deprivation has been shown to upregulate T3 levels in the hypothalamus in rats (22,25). However, no regulation of *Sned1* was observed in 48 hour food-deprived and re-fed rats. This might indicate that short-term regulation of mechanisms involved in food intake and energy homeostasis might engage different mechanisms than for longer-term regulation.

Hairless

Hairless encodes for a transcriptional regulator associated with thyroid hormone receptors and involved in the Wnt signaling pathway, playing a role in axon guidance and stem cell proliferation. *Hairless* has been described to be directly regulated by thyroid hormone in the developing brain of neonatal rats (63) and has been shown to increase Wnt signaling and thereby cell proliferation, by repressing Wise, an inhibitor of the Wnt pathway (64). A recent study has identified HAIRLESS as a histone demethylase whose target genes include those involved in transcription regulation, the cell cycle, and neural activity (65). The potential role in neurogenesis is relevant to energy balance in the context of the recent discovery for neuronal progenitor role of hypothalamic tanycytes, which proceed to differentiate to neurons expressing appetite regulatory peptides (66,67). In our experiment, *Hairless* was strongly upregulated after T3 injection in the ependymal layer of the third ventricle. In Siberian hamsters, *Hairless* expression was increased in the LD state, when T3 synthesis by ependymal cells of the hypothalamus is highest and therefore could relate to possible plastic changes in the hypothalamus, including cell proliferation and adult neurogenesis across the seasons (68). However, *Hairless* mRNA expression was not affected by fasting and re-feeding in Sprague Dawley rats, a difference that may reflect long- and short-term regulation of energy balance or hypothalamic plasticity.

Plunc

Palate, lung, and nasal epithelium carcinoma associated protein (PLUNC) encodes a secretory protein that has been described in the epithelia of the conducting airways in humans and mammals (69). The PLUNC proteins are part of the lipid transfer/lipopolysaccharide binding protein (LT/LBP) family, whose members PLTP, CETP, BPI, LBP, and PLUNC bind a variety of lipid substrates. Expression of *Plunc* mRNA was found within the neuropil of the ARC when expression was induced by T3. *Plunc* mRNA expression decreased in the subependymal layer upon fasting. This appears counter-intuitive, given that fasting induces a rise in hypothalamic T3 levels (22,25) and *Plunc* mRNA expression did not recover within 24 hours of re-feeding. This suggests a regulatory mechanism other than T3 is likely to be involved in the response of this gene to fasting. The role of PLUNC remains unidentified, but as a secreted protein with surfactant activity (68), expressed in the subependymal layer, a possible role for PLUNC in the hypothalamus may be related to the location of expression next to the third ventricle with access to cerebrospinal fluid. No *Plunc* mRNA expression was found in the Siberian hamster, which reveals either a species difference in the requirement for this protein or the function of PLUNC may be assumed by an alternative protein.

In conclusion, we have shown that hypothyroidism has a profound effect on growth. In addition to the impact on the thyroid hormone sensing mechanisms via changes in thyroid hormone deiodinases and TRH, we also found that mRNA expression for the thyroid hormone transporter *Mct8* is subject to regulation by T3 in rodents. In addition, for the first time in rodents, we show that expression of *Agrp*, a key component of the recognized hypothalamic energy balance homeostatic mechanism, can be regulated by T3. Microarray analysis of RNA extracted from the hypothalamus of hypothyroid versus hyperthyroid-T3-treated rats revealed hypothalamic genes that are regulated by T3. These genes require further investigation to understand their role at the interface between the input pathway of T3 and output pathways via the central nervous system, neuroendocrine axes, or other aspects of neurophysiology. Three genes identified and assessed in this study—*Sned1*, *Hairless*, and *Plunc*—were found to be altered by T3 in the hypothalamus and in *in vivo* models where the neuroendocrine axis is challenged by fasting or the environmental parameter of photoperiod exposure.

Acknowledgments

This work was supported by PIEF-GA-2009-235106 Marie Curie individual fellowship and HE 6383/1-1 Emmy-Noether fellowship to Annika Herwig and further funding from the Scottish Government Rural and Environment Science and Analytical Services Division. We thank Jenny Morris and Pete Hedley of the Genome Technology group, James Hutton Institute, Dundee, for help in scanning the Agilent arrays, Dana Wilson for laboratory assistance, and Vivian Buchan and Donna Henderson for analysis of serum concentrations of glucose, NEFAs, and triglycerides.

Author Disclosure Statement

The authors have nothing to declare.

References

1. Lechan RM, Fekete C 2006 The TRH neuron: a hypothalamic integrator of metabolism. Prog Brain Res **153:**209–235.
2. Tata JR EL, Suranyi EM 1962 Interaction between thyroid hormones and cellular constituents. I. Binding to isolated sub-cellular particles and subparticulate fractions. Biochim Biophys Acta **60:**461–479.
3. Tata JR 1963 Inhibition of the biological action of thyroid hormones by actinomycin D and puromycin. Nature **197:** 1167–1168.
4. Krotkiewski M 2002 Thyroid hormones in the pathogenesis and treatment of obesity. Eur J Pharmacol **440:**85–98.
5. Dale J, Daykin J, Holder R, Sheppard MC, Franklyn JA 2001 Weight gain following treatment of hyperthyroidism. Clin Endocrinol **55:**233–239.
6. Brunova J, Bruna J, Joubert G, Koning M 2003 Weight gain in patients after therapy for hyperthyroidism. Samj S Afr Med J **93:**529–531.
7. Roos A, Bakker SJL, Links TP, Gans ROB, Wolffenbuttel BHR 2007 Thyroid function is associated with components of the metabolic syndrome in euthyroid subjects. J Clin Endocr Metab **92:**491–496.

8. Bianco AC, Maia AL, da Silva WS, Christoffolete MA 2005 Adaptive activation of thyroid hormone and energy expenditure. Bioscience Rep **25:**191–208.
9. Silva JE 2006 Thermogenic mechanisms and their hormonal regulation. Physiol Rev **86:**435–464.
10. Herwig A, Ross AW, Nilaweera KN, Morgan PJ, Barrett P 2008 Hypothalamic thyroid hormone in energy balance regulation. Obesity Facts **1:**71–79.
11. Coppola A, Liu ZW, Andrews ZB, Paradis E, Roy MC, Friedman JM, Ricquier D, Richard D, Horvath TL, Gao XB, Diano S 2007 A central thermogenic-like mechanism in feeding regulation: An interplay between arcuate nucleus T3 and UCP2. Cell Metab **5:**21–33.
12. Klieverik LP, Janssen SF, van Riel A, Foppen E, Bisschop PH, Serlie MJ, Boelen A, Ackermans MT, Sauerwein HP, Fliers E, Kalsbeek A 2009 Thyroid hormone modulates glucose production via a sympathetic pathway from the hypothalamic paraventricular nucleus to the liver. P Natl Acad Sci USA **106:**5966–5971.
13. Lopez M, Varela L, Vazquez MJ, Rodriguez-Cuenca S, Gonzalez CR, Velagapudi VR, Morgan DA, Schoenmakers E, Agassandian K, Lage R, de Morentin PBM, Tovar S, Nogueiras R, Carling D, Lelliott C, Gallego R, Oresic M, Chatterjee K, Saha AK, Rahmouni K, Dieguez C, Vidal-Puig A 2010 Hypothalamic AMPK and fatty acid metabolism mediate thyroid regulation of energy balance. Nat Med **16:**1001–1097.
14. Dratman MB, Crutchfield FL, Schoenhoff MB 1991 Transport of iodothyronines from blood-stream to brain—contributions by blood–brain and choroid–plexus cerebrospinal-fluid barriers. Brain Res **554:**229–236.
15. Friesema ECH, Ganguly S, Abdalla A, Fox JEM, Halestrap AP, Visser TJ 2003 Identification of monocarboxylate transporter 8 as a specific thyroid hormone transporter. J Biol Chem **278:**40128–40135.
16. Sugiyama D, Kusuhara H, Taniguchi H, Ishikawa S, Nozaki Y, Aburatani H, Sugiyama Y 2003 Functional characterization of rat brain-specific organic anion transporter (Oatp14) at the blood–brain barrier. High affinity transporter for thyroxine (vol 278, pg 43489, 2003). J Biol Chem **278:**49662–49662.
17. Fekete C, Lechan RM 2007 Negative feedback regulation of hypophysiotropic thyrotropin-releasing hormone (TRH) synthesizing neurons: role of neuronal afferents and type 2 deiodinase. Front Neuroendocrin **28:**97–114.
18. Baqui MMA, Gereben B, Harney JW, Larsen PR, Bianco AC 2000 Distinct subcellular localization of transiently expressed types 1 and 2 iodothyronine deiodinases as determined by immunofluorescence confocal microscopy. Endocrinology **141:**4309–4312.
19. Bianco AC, Salvatore D, Gereben B, Berry MJ, Larsen PR 2002 Biochemistry, cellular and molecular biology, and physiological roles of the iodothyronine selenodeiodinases. Endocr Rev **23:**38–89.
20. Barrett P, Ebling FJP, Schuhler S, Wilson D, Ross AW, Warner A, Jethwa P, Boelen A, Visser TJ, Ozanne DM, Archer ZA, Mercer JG, Morgan PJ 2007 Hypothalamic thyroid hormone catabolism acts as a gatekeeper for the seasonal control of body weight and reproduction. Endocrinology **148:**3608–3617.
21. Herwig A, Wilson D, Logie TJ, Boelen A, Morgan PJ, Mercer JG, Barrett P 2009 Photoperiod and acute energy deficits interact on components of the thyroid hormone system in hypothalamic tanycytes of the Siberian hamster (vol 296, pg R1307, 2009). Am J Physiol Reg I **297:** R1624–R1624.
22. Diano S, Naftolin F, Goglia F, Horvath TL 1998 Fasting-induced increase in type II iodothyronine deiodinase activity and messenger ribonucleic acid levels is not reversed by thyroxine in the rat hypothalamus. Endocrinology **139:** 2879–2884.
23. Fekete C, Gereben B, Doleschall M, Harney JW, Dora JM, Bianco AC, Sarkar S, Liposits Z, Rand W, Emerson C, Kacskovics I, Larsen PR, Lechan RM 2004 Lipopolysaccharide induces type 2 iodothyronine deiodinase in the mediobasal hypothalamus: Implications for the nonthyroidal illness syndrome. Endocrinology **145:**1649–1655.
24. Coppola A, Meli R, Diano S 2005 Inverse shift in circulating corticosterone and leptin levels elevates hypothalamic deiodinase type 2 in fasted rats. Endocrinology **146:**2827–2833.
25. Coppola A, Hughes J, Esposito E, Schiavo L, Meli R, Diano S 2005 Suppression of hypothalamic deiodinase type II activity blunts TRH mRNA decline during fasting. FEBS Lett **579:**4654–4658.
26. Boelen A, Kwakkel J, Wiersinga WM, Fliers E 2006 Chronic local inflammation in mice results in decreased TRH and type 3 deiodinase mRNA expression in the hypothalamic paraventricular nucleus independently of diminished food intake. J Endocrinol **191:**707–714.
27. Costa-e-Sousa RH, Hollenberg AN 2012 Minireview: the neural regulation of the hypothalamic-pituitary-thyroid axis. Endocrinology **153:**4128–4135.
28. Warner A, Mittag J 2012 Thyroid hormone and the central control of homeostasis. J Mol Endocrinol **49:**R29–R35.
29. Sjogren M, Alkemade A, Mittag J, Nordstrom K, Katz A, Rozell B, Westerblad H, Arner A, Vennstrom B 2007 Hypermetabolism in mice caused by the central action of an unliganded thyroid hormone receptor a1. Embo J **26:**4535–4545.
30. Bradley DJ, Young WS, 3rd, Weinberger C 1989 Differential expression of alpha and beta thyroid hormone receptor genes in rat brain and pituitary. Proc Natl Acad Sci U S A **86:**7250–7254.
31. Alkemade A, Vuijst CL, Unmehopa UA, Bakker O, Vennstrom B, Wiersinga WM, Swaab DF, Fliers E 2005 Thyroid hormone receptor expression in the human hypothalamus and anterior pituitary. J Clin Endocrinol Metab **90:**904–912.
32. Wiersinga WM, Chopra IJ 1982 Radioimmunoassays of thyroxine-(T4), 3,5,3′-triiodothyronine (T3), 3,3′,5′-triiodothyronine (Reverse T3, Rt3), and 3,3′-diiodothyronine (T2). Method Enzymol **84:**272–303.
33. Pohlenz J, Maqueem A, Cua K, Weiss RE, Van Sande J, Refetoff S 1999 Improved radioimmunoassay for measurement of mouse thyrotropin in serum: strain differences in thyrotropin concentration and thyrotroph sensitivity to thyroid hormone. Thyroid **9:**1265–1271.
34. Edgar R, Domrachev M, Lash AE 2002 Gene expression omnibus: NCBI gene expression and hybridization array data repository. Nucleic Acids Res **30:**207–210.
35. Ebling FJP, Wilson D, Wood J, Hughes D, Mercer JG, Morgan PJ, Barrett P 2008 The thyrotropin-releasing hormone secretory system in the hypothalamus of the Siberian hamster in long and short photoperiods. J Neuroendocrinol **20:**576–586.
36. Mercer JG, Lawrence CB, Beck B, Burlet A, Atkinson T, Barrett P 1995 Hypothalamic NPY and prepro-NPY mRNA

in Djungarian hamsters: effects of food deprivation and photoperiod. Am J Physiol **269:**R1099–R1106.
37. Mercer JG, Moar KM, Ross AW, Hoggard N, Morgan PJ 2000 Photoperiod regulates arcuate nucleus POMC, AGRP, and leptin receptor mRNA in Siberian hamster hypothalamus. Am J Physiol **278:**R271–R281.
38. Villafuerte BC, Phillips LS, Rane MJ, Weidong Z 2004 Insulin-response element binding protein 1. J Biol Chem **279:**36650–36659.
39. Villafuerte BC, Kaytor EN 2006 An insulin-response element-binding protein that ameliorates hyperglycemia in diabetes. J Biol Chem **280:**20010–20020.
40. Villafuerte BC, Barati MT, Song Y, Moore JP, Epstein PN, Portillo J 2009 Transgenic expression of insulin-response element binding protein-1 in β-cells reproduces type 2 diabetes. Endocrinology **150:**2611–2617.
41. Chahal J, Chen C-C, Rane MJ, Moore JP, Barati MT, Song Y Vilafuerte BC 2008 Regulation of insulin-response element binding protein-1 in obesity and diabetes: potential role in impaired insulin-induced gene transcription. Endocrinology **149:**4829–4836.
42. Hervas F, Morreale de Escobar G, Escobar Del Rey F 1975 Rapid effects of single small doses of L-thyroxine and triiodo-L-thyronine on growth hormone, as studied in the rat by radioimmunoassy. Endocrinology **97:**91–101.
43. Larsen PR, Frumess RD 1977 Comparison of the biological effects of thyroxine and triiodothyronine in the rat. Endocrinology **100:**980–988.
44. Del Prato S, Tiengo A 2001 The importance of first-phase insulin secretion: implications for the therapy of type 2 diabetes mellitus. Diabetes Metab Res Rev **17:**164–174.
45. Pizzagalli F, Hagenbuch B, Stieger B, Klenk U, Folkers G, Meier PJ 2002 Identification of a novel human organic anion transporting polypeptide as a high affinity thyroxine transporter. Mol Endocrinol **16:**2283–2296.
46. Westholm DE, Stenehjem DD, Rumbley JN, Drewes LR, Anderson GW 2009 Competitive inhibition of organic anion transporting polypeptide 1c1-mediated thyroxine transport by the fenamate class of nonsteroidal antiinflammatory drugs. Endocrinology **150:**1025–1032.
47. Kinne A, Schulein R, Krause G 2011 Primary and secondary thyroid hormone transporters. Thyroid Res **4:**S7.
48. Fonseca TL, Correa-Medina M, Campos MP, Wittmann G, Werneck-de-Castro JP, Arrojo e Drigo R, Mora-Garzon M, Ueta CB, Caicedo A, Fekete C, Gereben B, Lechan RM, Bianco AC 2013 Coordination of hypothalamic and pituitary T3 production regulates TSH expression. J Clin Invest **123:**1492–1500.
49. Sharlin DS, Gilbert ME, Taylor MA, Ferguson DC, Zoeller RT 2010 The nature of the compensatory response to low thyroid hormone in the developing brain. J Neuroendocrinol **22:**153–165.
50. Fan W, Boston BA, Kesterson RA, Hruby VJ, Cone RD 1997 Role of melanocortinergic neurons in feeding and the agouti obesity syndrome. Nature **385:**165–168.
51. Kim MS, Small CJ, Stanley SA, Morgan DG, Seal LJ, Kong WM, Edwards CM, Abusnana S, Sunter D, Ghatei MA, Bloom SR 2000 The central melanocortin system affects the hypothalamo-pituitary thyroid axis and may mediate the effect of leptin. J Clin Invest **105:**1005–1011.
52. Wirth MM, Olszewski PK, Yu C, Levine AS, Giraudo SQ 2001 Paraventricular hypothalamic alpha-melanocyte-stimulating hormone and MTII reduce feeding without causing aversive effects. Peptides **22:**129–134.
53. Clark JT, Kalra PS, Kalra SP 1985 Neuropeptide Y stimulates feeding but inhibits sexual behavior in rats. Endocrinology **117:**2435–2442.
54. Ollmann MM, Wilson BD, Yang YK, Kerns JA, Chen Y, Gantz I, Barsh GS 1997 Antagonism of central melanocortin receptors *in vitro* and *in vivo* by agouti-related protein. Science **278:**135–138.
55. Rossi M, Kim MS, Morgan DG, Small CJ, Edwards CM, Sunter D, Abusnana S, Goldstone AP, Russell SH, Stanley SA, Smith DM, Yagaloff K, Ghatei MA, Bloom SR 1998 A C-terminal fragment of Agouti-related protein increases feeding and antagonizes the effect of alpha-melanocyte stimulating hormone in vivo. Endocrinology **139:**4428–4431.
56. Hagan MM, Rushing PA, Pritchard LM, Schwartz MW, Strack AM, Van Der Ploeg LH, Woods SC, Seeley RJ 2000 Long-term orexigenic effects of AgRP-(83—132) involve mechanisms other than melanocortin receptor blockade. Am J Physiol Regul Integr Comp Physiol **279:**R47–52.
57. Gropp E, Shanabrough M Borok E, Xu AW, Janoschek R, Buch T, Plum T, Balthasar N, Hampel B, Waisman A, Barsh GS, Horvath TL, Bruning JC 2005 Agouti-related peptide-expressing neurons are mandatory for feeding Nat Neurosci **8:**1289–1291.
58. Byerly MS, Simon J, Lebihan-Duval E, Duclos MJ, Cogburn LA, Porter TE 2009 Effects of BDNF, T3, and corticosterone on expression of the hypothalamic obesity gene network *in vivo* and *in vitro*. Am J Physiol Regul Integr Comp Physio **296:**R1180–1189.
59. Ross AW, Johsson CE, Bell LM, Reilly L, Duncan JS, Barrett P, Heideman PD, Morgan PJ 2009 Divergent regulation of hypothalamic neuropeptide Y and agouti-related peptide protein by photoperiod in F344 rats with differential food intake and growth. J Neuroendocrinol **21:**610–619.
60. Calvo R, Obregon MJ, Ruiz de Ona C, Escobar del Rey F, Morreale de Escobar G 1990 Congenital hypothyroidism, as studied in rats. Crucial role of maternal thyroxine but not of 3,5,3′-triiodothyronine in the protection of the fetal brain. J Clin Invest **86:**889–899.
61. Sanders NM, Dunn-Meynell AA, Levin BE 2004 Third ventricular alloxan reversibly impairs glucose counterregulatory responses. Diabetes **53:**1230–1236.
62. Frayling C, Britton R, Dale N 2011 ATP-mediated glucosensing by hypothalamic tanycytes. J Physiol **589:**2275–2286.
63. Potter GB, Zarach JM, Sisk JM, Thompson CC 2002 The thyroid hormone-regulated corepressor hairless associates with histone deacetylases in neonatal rat brain. Mol Endocrinol **16:**2547–2560.
64. Thompson CC, Sisk JM, Beaudoin GM 3rd 2006 Hairless and Wnt signaling: allies in epithelial stem cell differentiation. Cell Cycle **5:**1913–1917.
65. Liu L, Kim H, Casta A, Kobayashi Y, Shapiro LS, Christiano AM 2014 Hairless is a histone H3K9 demethylase. FASEB J **28:**1534–1542.
66. Haan N, Goodman T, Najdi-Samiei A, Stratford CM, Rice R, El Agha E, Bellusci S, Hajihosseini MK 2013 Fgf10-expressing tanycytes add new neurons to the appetite/energy-balance regulating centers of the postnatal and adult hypothalamus. J Neurosci **33:**6170–6180.
67. Lee DA, Bedont JL, Pak T, Wang H, Song J, Miranda-Angulo A, Takiar V, Charubhumi V, Balordi F, Takebayashi H, Aja S, Ford E, Fishell G, Blackshaw S 2012

Tanycytes of the hypothalamic median eminence form a diet-responsive neurogenic niche. Nature neuroscience **15:**700–702.
68. Ebling FJ, Barrett P 2008 The regulation of seasonal changes in food intake and body weight. J Neuroendocrinol **20:**827–833.
69. Gakhar L, Bartlett JA, Penterman J, Mizrachi D, Singh PK, Mallampalli RK, Ramaswamy S, McCray PB Jr. 2010 PLUNC is a novel airway surfactant protein with anti-biofilm activity. PloS One **5:**e9098.

Address correspondence to:
Perry Barrett, PhD
Rowett Institute for Nutrition and Health
University of Aberdeen
Greenburn Road
Bucksburn
Aberdeen AB21 9SB
United Kingdom

E-mail: p.barrett@abdn.ac.uk